

# Detection of Defects in Ferromagnetic Materials by Nanofluid as a Sensor

RoshniC.A<sup>1</sup>, ShanthaSelvakumari S<sup>2</sup>

<sup>1</sup>Student, Centre of Nano Science & Technology, Dept. of Mechanical Engineering, Mepco Schlenk Engineering College, Sivakasi, TamilNadu.

<sup>2</sup>Professor&Head, Dept. of Electronics & Commn Engg, Mepco Schlenk Engineering College, Sivakasi, TamilNadu, India

**ABSTRACT:** Nanotechnology provides wide range of applications in medicine, electronics, energy production and biomaterial fields. One of the applications used in this project is magnetic flux leakage sensor to detect the defects in ferromagnetic material. Magnetic Flux Leakage is one of the most widely used electromagnetic non-destructive techniques to locate and asses discontinuities such as fatigue, cracks, corrosion, erosion, non-metallic inclusion and abrasive wear in magnetic components. The gradient in the magnetic flux lines around the defective region induces the formation of one-dimensional array of nano-particles along the field direction in the Nano fluid, which produces a discernible grey level contrast in the Ferro fluid. The grey level contrast produced by the leaked magnetic flux is used to detect the defects buried inside the sample. Small defects provide shape information on the defects because of its high sensitivity and spatial resolution. Different metal oxide (Nickel oxide, Iron oxide and Ferrofluid) nanofluids were prepared and characterized using SEM, AFM and FTIR. Using VSM technique, the magnetization, coercivity and paramagnetic nature of nanofluids are studied. Ferrofluid shows super-paramagnetic behavior with enhanced coercivity and magnetization when compared to other fluids.

**KEYWORDS:** Non-destructive testing, Magnetic flux leakage, Coercivity, Magnetic behavior.

## 1. INTRODUCTION

Magnetic nano fluid are colloidal suspensions of super-paramagnetic particles in a suitable carrier fluid. Magnetic nanofluids have attracted enormous interest in recent years

because of their field driven self-assembly and tunable properties. The unique field driven properties of magnetic nanofluids have been exploited for several interesting applications such as electronics, cooling, sealant, dampers, optical filter, defect and ion sensors etc. Using the magnetically tunable optical properties of nano-emulsions, we have developed an optical probe for defect detection in ferromagnetic materials. In this work, we report a methodology to image defects in ferromagnetic materials and components using magnetic nano-fluids and the defect feature extraction and its quantification using image enhancing methods.

Magnetic flux leakage is one of the most commonly used electromagnetic nondestructive techniques (NDT). This technique has been extensively used in metal industries, to locate and asses the discontinuities such as fatigue, cracks, corrosion, erosion, non-metallic inclusion and abrasive wear in ferro-magnetic structures. MFL technique is found to have a high degree of certainty in the detection of defects with better sensitivity. The partial ferrite structure formed in this material, due to their imperfect heat treatments and mechanical stress are often wrongly diagnosed as a crack and sometimes real cracks are misjudged as ferrite, which can lead to catastrophic failures of engineering components. Lack of magnetization and over saturation of materials can leads to a poor flux leakage signal and overlap of signals with large background. For better visualization of the defects, the excitation flux should be sufficient to penetrate the defect depth and homogeneous throughout the specimen. The lift off distance of the sensor should be adjusted such that the defect signal is strong enough to detect distinctly from the background noise. These problems associated with conventional MFL techniques warrant the need to have more reliable, simple, cost effective and sensitive

## Detection of Defects in Ferromagnetic Materials by Nanofluid as a Sensor

techniques for detection of leakage magnetic flux in ferromagnetic components and structures.

repeatedly with de-ionized water, and then calcined into  $Fe_2O_3$ .

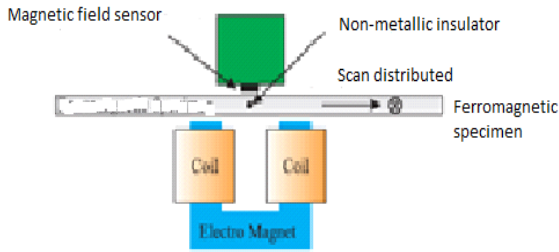
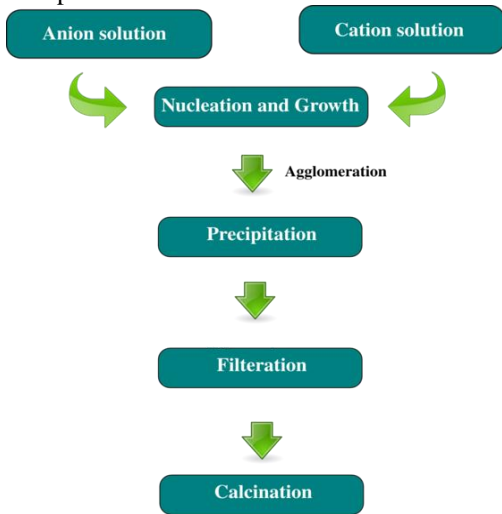


Fig 1: Schematic experimental setup for MFL testing.

## II. MATERIALS AND METHODS

Co-Precipitation is the incorporation of trace element into mineral structure during solid solution formation and re-crystallization of minerals. This Process will reduce the mobility and toxicity of toxic trace elements that are incorporated in the mineral.



### 2.1 Synthesis of $Fe_2O_3$ nano particle

Iron ore tailings were weighed (100 g), and mixed with 37.5wt% hydrochloric acid (HCl). Then pickling was filtered out and collected. An appropriate amount of hydrogen peroxide ( $H_2O_2$ ) was added to the filtrate so that all iron could exist in the  $Fe^{3+}$  form. Filtrate was heated to 60 °C, and its pH value was adjusted to 3.2 by adding an appropriate amount of concentrated ammonia. As a result, Fe was separated from tailings and precipitated into  $Fe(OH)_3$ . Finally, some amount of  $Fe(OH)_3$  was washed

### 2.2 Synthesis of $Fe_3O_4$ nano particle

Iron hydroxide solve with acid to get  $FeCl_3$ . Iron sulphate was mixed iron chloride and sodium hydroxide was added drop-wise.  $Fe_3O_4$  precipitate was aged at 65 degree for 30 min in ultrasonic water bath. To purify prepared  $Fe_3O_4$  particles, the samples were washed repeatedly with de-ionized water and ethanol until pH level of was reached. Particles were then dired at 74 degree in vaccum to get  $Fe_3O_4$ .

### 2.3 Preparation of colloidal magnetic nanoparticles

Dissolved 23.5g ferrous chloride and 8.6 g  $FeCl_2 \cdot 4H_2O$  in 600ml de-ionized water under  $N_2$  with mechanical stirring at 600 rpm (revolution per minute ) and 85°C and then quickly added 30 ml of 7.1M  $NH_4OH$ . To the resulting suspension 16ml oleic acid was added drop-wise over a period of 30 min. After several minutes, the magnetic precipitate was separated by magnetic decantation and washed with de-ionized water several times, two times with ethanol and finally evaporated to dryness to get iron oxide ( $Fe_3O_4$ ) powder. It was further modified with 4 ml of 7.1 M  $NH_4OH$  to form the hydrophilic magnetic nanoparticles and leading to a stable colloidal dispersion (pH 7) after repeated washing.

## 111. EXPERIMENTAL SETUP

### 3.1 Detection mechanism

The schematic overview of the detection mechanism of the magnetic scanning imaging method used to detect defects in a ferromagnetic specimen is shown in figure 1. A ferromagnetic specimen is magnetized by a permanent magnet. When there are no discontinuities of physical and chemical characteristics, defects, cracks, and so on, the distortion of magnetic lines of force over the specimen is not much, shown in figure (red circle). When there is a defect, the distortion of magnetic lines of force will be great, shown in figure (red circle). The defect region, considered as the air region, has great reluctance because its permeability is far less than that of the ferromagnetic specimen. Some magnetic lines of force, therefore, bypass the defect region and flow from the vicinity of ferromagnetic material.

# Detection of Defects in Ferromagnetic Materials by Nanofluid as a Sensor

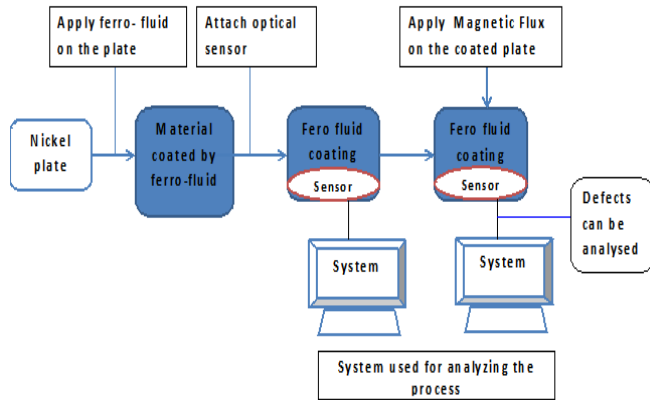


Fig 2: Block Diagram of Detecting Defects

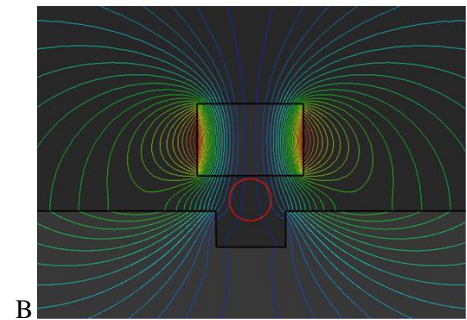
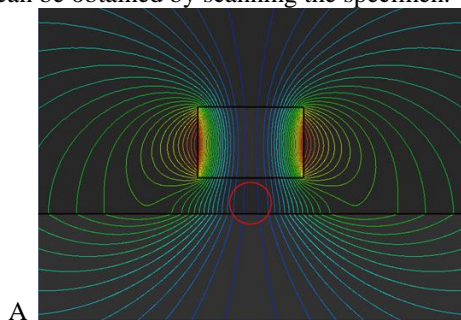
In this paper, the magnetization direction of the permanent magnet is perpendicular to the surface of the specimen, along the z-axis, and only the vertical component of the magnetic flux density,  $B_z$ , over the specimen is measured:

$$B_z = B_{zm} + B_z(1)$$

Where  $B_{zm}$  is the vertical component of the incident magnetic flux density produced by the permanent magnet, whose magnitude is almost constant, and  $B_z$  is the change of the magnetic flux density generated by the defect and eddy current in the ferromagnetic material:

$$B_z = B_{zg} - B_{ze} \quad (2)$$

Where  $B_{zg}$  is the change of the magnetic flux density due to the presence of the defect, and  $B_{ze}$  is the magnetic flux density produced by the eddy current induced in the ferromagnetic material when a permanent magnet moves over it. Combining a small permanent magnet producing the main magnetic field with the magnetometer measuring the vertical components of the magnetic flux density  $B_z$  over the ferromagnetic material, the two-dimensional images of magnetic field fluctuations caused by defects can be obtained by scanning the specimen.



## 4. RESULTS AND DISCUSSION

### 4.1 Characteristics of $Fe_2O_3$

#### 4.1.1 AFM image

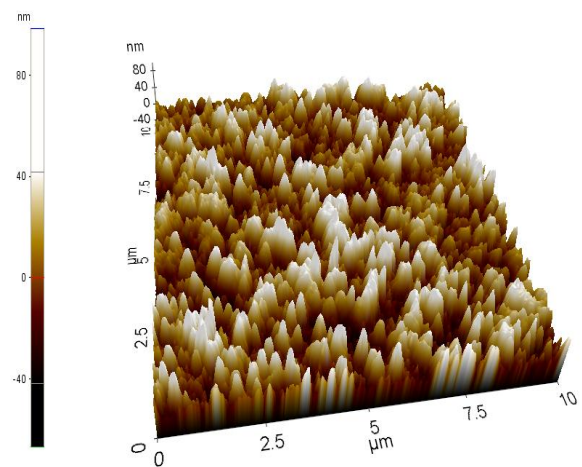


Fig.3: AFM image  $Fe_2O_3$

The 3D image shows the synthesized iron oxide using co-precipitation method. The topography image obtained from AFM for iron oxide nano-particles increase in particle size for the increase in temperature which ranges from 500 to 800 degree Celsius. The particle size is about 60-80 nm.

#### 4.1.2 Scanning Electron Microscope analysis

The SEM analysis is carried out by using Hitachi SUI510, scanning electron microscope.

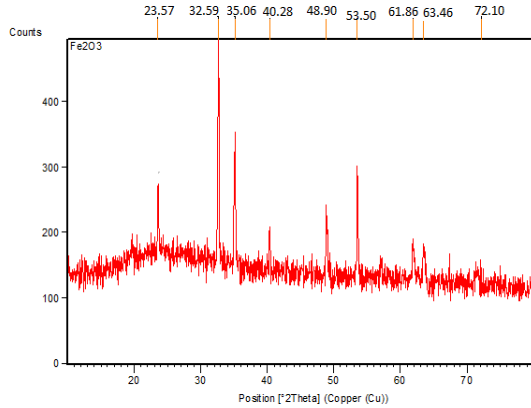


Fig.4: SEM image of Fe<sub>2</sub>O<sub>3</sub>

The image shows the mono dispersed and uniform size of the particles arranged with spherical shape in nature with a diameter of around 100-200nm. The SEM image shows the particle size and reveals the presence and uniformity of the distributed particles.

#### 4.1.3 FTIR analysis

The FT-IR spectra Fe<sub>2</sub>O<sub>3</sub> is shown in the Fig 4.1.3. The peak value becomes 550cm<sup>-1</sup> that corresponds to a strong adsorption band of Fe-O stretching vibrations and the other one at 650 cm<sup>-1</sup> region is due to the O-H stretching vibration of the Fe<sup>3+</sup>-O stretching vibration.

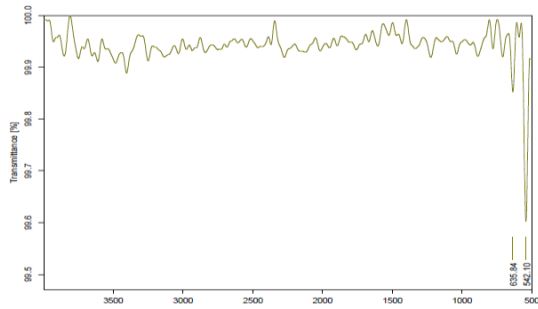


Fig 5 FTIR analysis for Fe<sub>2</sub>O<sub>3</sub>

#### 4.1.4 X-ray Diffraction analysis:

The structural features of Iron oxide are explored from XRD data. The XRD pattern of final powders revealed well developed reflection of Fe<sub>2</sub>O<sub>3</sub> nanoparticle (JCPDS.No. 89-8104).



Fig 6 XRD analysis of Fe<sub>2</sub>O<sub>3</sub>

The XRD pattern of the sample exhibits the characteristics peak at 2 $\Theta$  = 24.213°, which corresponds to the (012) plane. It also exhibits peaks at 2 $\Theta$  = 33.255°, 2 $\Theta$  = 35.722° are indexed as planes (104), (110) respectively. The peak at 2 $\Theta$  = 39.408° which corresponds to the (006) plane confirms the presence of Fe<sub>2</sub>O<sub>3</sub> nanoparticle.

#### 4.2 Characterization of Fe<sub>3</sub>O<sub>4</sub> nanoparticles

##### 4.2.1 AFM image:

The 3D image shows the synthesized iron oxide using co-precipitation method.

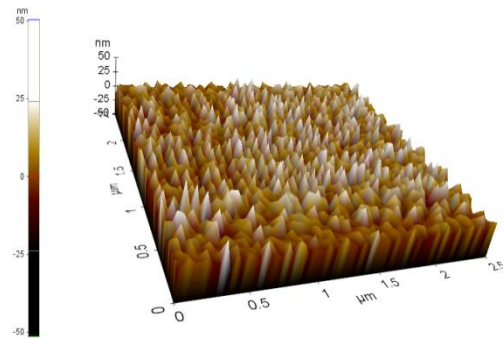


Fig 7 AFM image of Fe<sub>3</sub>O<sub>4</sub>

The topography image obtained from AFM for iron oxide nano-particles increase in particle size for the increase in temperature which ranges from 500 to 800degree Celsius. The particle size is about 60-80 nm.

**4.2.2 SEM image:**

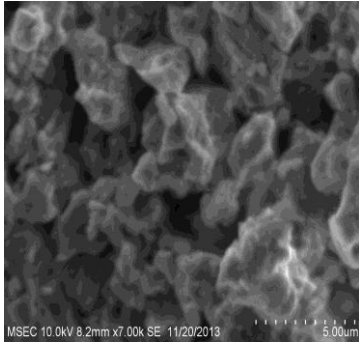


Fig 8: SEM image of Fe<sub>3</sub>O<sub>4</sub>

SEM image shows the particle size and reveals the presence and uniformity of the distributed particles. It was clear that the particles obtained were in nano size ranging in the diameter from 100-200nm. The SEM image shows the particle size and reveals the presence and uniformity of the distributed particles..

**4.2.3 FTIR analysis:**

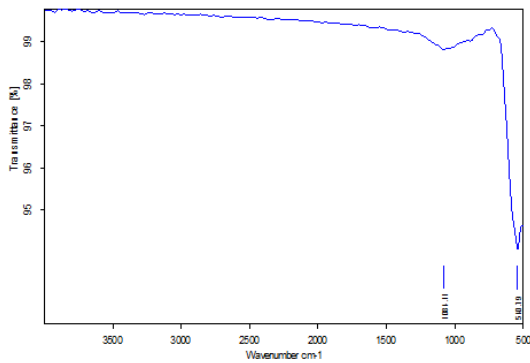


Fig. 9: FTIR image of Fe<sub>3</sub>O<sub>4</sub>

The FT-IR spectra Fe<sub>3</sub>O<sub>4</sub> is shown in the Fig 4.2.3. The sample exhibits two strong peaks in the range of 100-510 cm<sup>-1</sup> corresponding to the vibrational energies of Fe-O bond. The peak value becomes 550cm<sup>-1</sup> that corresponds to a strong adsorption band of Fe-O stretching vibrations and the other one at 650 cm<sup>-1</sup> region is due to the O-H stretching vibration of the Fe<sup>3+</sup>O stretching vibration.

**4.2.4. VSM analysis:**

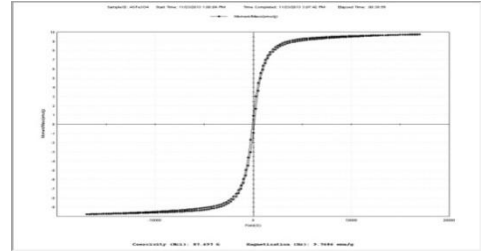


Fig. 10 : VSM analysis for Fe<sub>3</sub>O<sub>4</sub>

Fig: 10 shows the magnetization value is 9.768emu/g and the coercivity value becomes 87.697g. Magnetic properties of Fe<sub>3</sub>O<sub>4</sub> nanoparticles were measured by VSM at 300 K. No magnetic hysteresis loop appears in magnetization curve of Fe<sub>3</sub>O<sub>4</sub> nanoparticles, exhibiting super-paramagnetism.

**4.3 Characterization of colloidal magnetic nanoparticles:**

**4.3.1 SEM image:**

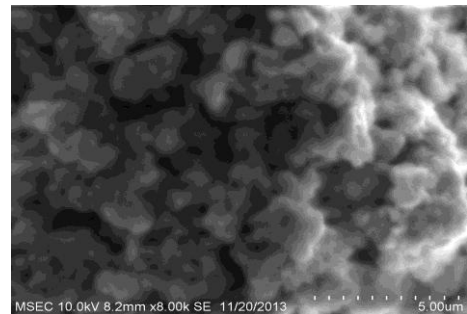


Fig 11 SEM image of magnetic nanoparticles

SEM image shows the particle size and reveals the presence and uniformity of the distributed particles. SEM image shows the particle size and reveals the presence and uniformity of the distributed particles. It was clear that the particles obtained were in nano size ranging in the diameter from 100-200nm. The SEM image shows the particle size and reveals the presence and uniformity of the distributed particles

**4.3.2 FTIR analysis:**

The FT-IR spectra colloidal magnetic nanoparticles shown in the Fig12 The sample exhibits two strong peaks in the range of 490-501 cm<sup>-1</sup> corresponding to the vibrational energies of Fe-O bond. The FTIR spectra of the iron oxide nanoparticles



## Detection of Defects in Ferromagnetic Materials by Nanofluid as a Sensor

and micro gel magnetic particles. It was reported that the characteristic absorption band of Fe–O bond of bulk Fe<sub>3</sub>O<sub>4</sub> was at 570 and 375 cm<sup>-1</sup>.

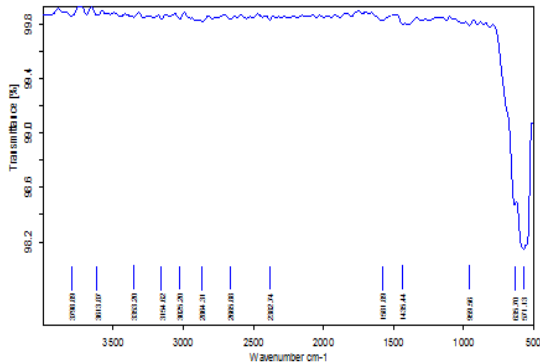


Fig 12: FTIR analysis of magnetic nanoparticles

### 4.3.3 VSM analysis:

The magnetization value is 29.59emu/g and the coercivity value becomes 1.1818g.

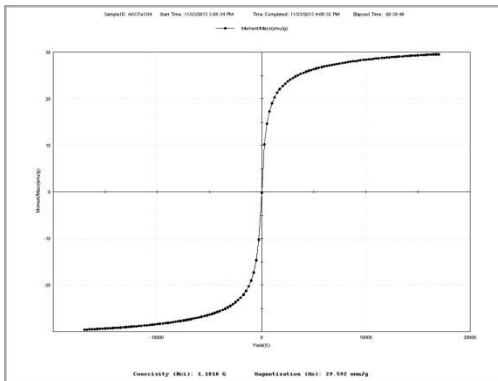


Fig.13: VSM image of Colloidal magnetic nanoparticles

It is also without hysteresis, and no sign of finite coercivity field and remnant magnetization can be found from the curve. From the magnetization curve, we can also see that the magnetization does not saturate at 11000 Oe magnetic fields.

### Performance Analysis:

Methods	Magnetization Value(emu/g)	Coercivity(g)
Emulsion method	22.6	67.697
Co-Precipitation method for Fe <sub>3</sub> O <sub>4</sub>	9.7686	87.697
Co-Precipitation method for Colloidal Magnetic Nanoparticle	29.592	1.1818

Here the first value of magnetization is higher when compare to other values. But the uniformity good in other two magnetization values. The defects are easily shown by the help of magnetic flux leakage sensor. There are possibilities to further improve the sensitivity by using emulsions with improved stabilization and also with enhanced magnetization fields.

## V.CONCLUSION

Nanometer sized Fe<sub>3</sub>O<sub>4</sub> and colloidal magnetic nanoparticles were prepared by co-precipitation process. The morphological structure and properties of nanoparticles were characterized by using SEM, AFM, VSM, XRD and FTIR analysis to determine the purity and of the particles. Compare to other nanofluids, ferrofluids has good efficiency, magnetization value and the defect can be easily identified in the ferromagnetic materials. The advantage of the nanofluids sensor is that it is simple, in-expensive and covers large area inspection in a short period of time.

## ACKNOWLEDGEMENT

This work was supported by Centre for nanoscience and Technology, Mepco Schlenk Engineering college, Sivakas

## REFERENCES

- [1] V.Mahendran et al (2013), "Naked eye visualization of defects in ferromagnetic materials and components" NDT & E international-1535
- [2] R.AncyBeautlin et al (2013), "Magnetic Nanofluid Based approach for imaging defects", Journal of nanofluids vol.2, pp, 165-174.

- [3] J.Philip et al (2000), “A new optical technique for detection of defects in ferromagnetic materials and components”, *NDT & E International* 33, 289-295.
- [4] Kikuchi H et al (2011) “Feasibility study of application of MFL to monitoring of wall thinning under reinforcing plates in nuclear power plants”, *IEEE Trans on Magnetics*,47,3963-3966.
- [5] Chunyan Xiao et al (2011), “A method of magnetic scanning imaging for detecting defects in ferromagnetic materials”, *Measurement Science and Technology*, 22, 025503(7).
- [6] M.Ravan et al (2010),”Nanofluid based optical sensor for rapid visual inspection of defects in ferromagnetic materials”, *IEEE Trans. Magn*,46(4),1024.
- [7] Wei Wu-Quanguo He-changzhong Jiang et al (2008) “Magnetic iron oxide nanoparticle: synthesis and surface functionalization strategies”, *Nanoscale Res Lett*, 3,397-415.
- [8] T.Nara et al (2007), “A sensor measuring the magnetic flux density for pipe crack detection using the Magnetic flux Leakage method”, *Appl.Phys.*109, 07E305.
- [9] Altschuler E et al (1995), “Nonlinear model of flaw detection in steel pipes by magnetic flux leakage”, *NDT and E International*, 28, 1995, 35-40
- [10] J.Blitz et al (1991), *Electrical and Magnetic methods of non-destructive testing*(Adam Hilger, Bristol, England)
- [11] BibetteJ et al (1991), “Depletion interactions and fractionated crystallization for poly-disperse emulsion purification”, *Journal Colloid Interface Science*, 147, 474-478.
- [12] Forster F et al (1986), “New findings in the field of non-destructive magnetic leakage field inspection”, *NDT Int.*19, 3-14.
- [13] Shen Wu et al (2011), “Fe<sub>3</sub>O<sub>4</sub> magnetic nanoparticles synthesis from tailings by ultrasonic chemical co-precipitation,” *Materials Letters* 65,1882–1884
- [14] Aslam Khan et al (2008), “Preparation and characterization of magnetic nanoparticles embedded in microgels”, *Materials Letters* 62,898–902
- [15] G.A. van Ewijk et al (1999), “Convenient preparation methods for magnetic colloids”, *Magnetism and magnetic materials* 201, 31-33.